

UCSF

UC San Francisco Previously Published Works

Title

Neocortical integration of transplanted GABA progenitor cells from wild type and GABAB receptor knockout mouse donors

Permalink

<https://escholarship.org/uc/item/5q53f266>

Authors

Sebe, Joy Y
Looke-Stewart, Elizabeth
Dinday, Matthew T
[et al.](#)

Publication Date

2014-02-01

DOI

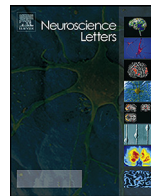
10.1016/j.neulet.2013.11.012

Peer reviewed



Contents lists available at ScienceDirect

Neuroscience Letters

journal homepage: www.elsevier.com/locate/neulet

Neocortical integration of transplanted GABA progenitor cells from wild type and GABA_B receptor knockout mouse donors

Joy Y. Sebe^{a,*}, Elizabeth Looke-Stewart^a, Matthew T. Dinday^a, Arturo Alvarez-Buylla^{a,b,c}, Scott C. Baraban^{a,b,c}

^a Department of Neurological Surgery, University of California, San Francisco, San Francisco, CA 94143, United States

^b Graduate Program in Neuroscience, University of California, San Francisco, San Francisco, CA 94143, United States

^c The Eli and Edythe Broad Center of Regeneration Medicine and Stem Cell Research, University of California, San Francisco, San Francisco, CA 94143, United States

HIGHLIGHTS

- Transplantation of MGE progenitor cells into neocortex generates new inhibitory interneurons.
- Inhibitory interneurons derived from MGE progenitor cells preferentially distribute in neocortical layers 2/3, 5 and 6.
- Functional GABA_B receptors are not required for laminar positioning of MGE-derived interneurons following transplantation.

ARTICLE INFO

Article history:

Received 17 August 2013

Received in revised form 17 October 2013

Accepted 10 November 2013

Keywords:

Interneuron

GABA

Laminar

Neocortex

Transplantation

ABSTRACT

Most cortical interneurons originate in a region of the embryonic subpallium called the medial ganglionic eminence (MGE). When MGE cells are transplanted into cerebral cortex, these progenitors migrate extensively and differentiate into functional inhibitory neurons. Although MGE progenitors have therapeutic potential following transplantation, it is unknown precisely how these cells distribute within neocortical lamina of the recipient brain. Here we transplanted mouse embryonic day 12.5 MGE progenitors into postnatal neocortex and evaluated laminar distribution of interneuron subtypes using double- and triple-label immunohistochemistry. Studies were performed using wild type (WT) or donor mice lacking a metabotropic GABA_B receptor subunit (GABA_{B1}R KO). MGE-derived neurons from WT and GABA_{B1}R KO mice preferentially and densely distributed in neocortical layers 2/3, 5 and 6. As expected, MGE-derived neurons differentiated into parvalbumin+ and somatostatin+ interneurons within these neocortical lamina. Our findings provide insights into the anatomical integration of MGE-derived interneurons following transplantation.

© 2013 Published by Elsevier Ireland Ltd.

1. Introduction

Inhibitory interneurons, approximately 20% of all neurons in adult neocortex, play a critical role in regulating normal network excitability and behavior [1]. Interneurons are generated in the medial (~70%) and caudal (~20%) ganglionic eminences (MGE and CGE) and the preoptic area (~10%) then migrate tangentially to their final laminar positions in neocortex [2–6]. Transcription factors and ligand–receptor complexes, including Nkx2.1, sonic hedgehog and smoothened, are thought to regulate interneuron proliferation, differentiation and migration [7]. In addition, GABA, the primary inhibitory neurotransmitter in the central nervous system, may play a key role in interneuron development via actions

on GABA_A and GABA_B receptors (GABA_A and GABA_BRs) [8]. During embryonic development, GABA_AR-mediated depolarization promotes neuronal proliferation [9,10] and interneuron migration [11]. GABA_BRs are metabotropic receptors that inhibit the cell by activating K⁺ efflux and reducing presynaptic GABA release. GABA_BR subunits are expressed on migrating interneurons of the embryonic rat brain [12] and in vitro GABA_BR activation promotes migration and entry of MGE progenitor cells into developing neocortex [13–15]. Whether GABA_BRs play a role in regulating differentiation or laminar distribution of transplanted interneurons is unknown.

Recent studies suggest that interneurons derived from the MGE are organized into spatially isolated clusters [16]. Interneuron clustering within neocortex is most prominent for interneuron sub-types originating in the embryonic MGE e.g., parvalbumin+ and somatostatin+. Viral labeling of endogenous MGE-derived interneurons at embryonic day 11.5 and 14.5 demonstrated that

* Corresponding author. Tel.: +1 5102056602.
E-mail address: joysebe@gmail.com (J.Y. Sebe).

these cells consistently cluster in the infragranular or supragranular layers of neocortex [17]. Here, we examined the laminar distribution of transplanted MGE-derived interneuron progenitors obtained from wild type (WT) or knockout (KO) mice lacking a subunit of the GABA_B receptor (GABA_{B1}R). We isolated embryonic MGE progenitors at E12.5 and transplanted them into neocortex at postnatal day 3. Using antibodies recognizing specific interneurons sub-types we assessed laminar positioning of MGE-derived interneurons at postnatal days 30–40 e.g., a time when these cells become functionally integrated in the host brain [18].

2. Materials and methods

2.1. Animals

This study was carried out in strict accordance with the recommendations in the Guide for the Care and Use of Laboratory Animals of the National Institutes of Health. The protocol was approved by the Institutional Animal Care and Use Committee of the University of California (permit number: AN084339). GABA_{B1}R^{+/-} mice [19] (gift from Bernhard Bettler, University of Basel) were mated with actin-GFP⁺ mice to generate GABA_{B1}R^{+/-}:GFP and GABA_{B1}R^{-/-}:GFP, which we refer to as WT and GABA_{B1}R KO, respectively. GFP⁺ cells were transplanted into WT CD-1 mice (Charles River, Harlan).

2.2. Transplantation

The anterior portion of MGE was dissected from E12.5 GFP-expressing mouse embryos and placed in a mixture of L-15 media (UCSF Cell Culture Facility) and DNase (Qiagen, Valencia, CA). In all studies, GFP⁺ MGE cells were unilaterally injected into neocortices of postnatal day 3 (P3) WT CD-1 mice. A “single MGE” refers to the MGE tissue obtained from one hemisphere of the embryonic brain and is thereby half of the total MGE cells in a donor embryo. For all studies, a single MGE was front-loaded into an injection needle containing media (outer diameter 70–80 μm), the needle was positioned at approximately a 45° angle relative to the platform of the stereotaxic apparatus and injected ~700 μm deep into the somatosensory cortex to systematically target layer 6. Each host mouse received only the GABA progenitor cells in a single MGE of cells so that a single embryo provided enough GABA progenitor cells to transplant 2 recipient mice. A single pregnant mouse yielded 9–13 embryos. A tissue sample from each of these embryos was collected for genotyping and the MGE of all of these embryos were dissected and transplanted into donor mice. Only donor mice that received either GFP⁺ WT (GFP:GABA_{B1}R^{+/-}) or GABA_{B1}R KO (GFP:GABA_{B1}R^{-/-}) MGE cells were analyzed and mice receiving GFP⁺ heterozygous (GFP: GABA_{B1}R^{+/-}) MGE cells were sacrificed and not analyzed.

2.3. Cell counting

To count the number of living and dead cells in a single dissected MGE, we used two methods. First, we counted the number of living and dead dissected cells prior to loading cells into the injection needle. MGE were dissociated in media containing DNase, combined with equal parts trypan blue, and loaded into a hemocytometer. Using this method, there were 180,000–200,000 cells in each MGE and 80–90% of these cells were alive (144,000–180,000 cells). Second, we counted the number of cells after a single MGE had been loaded into the injection needle and all visible cells were ejected into a 100 μL drop of media. The total cell count and viability decreased after needle loading. After needle loading, we counted 138,000–142,000 cells in each MGE and 50–70% of these cells were alive. Therefore, for each MGE loaded into the needle, we estimate an injection of approximately 69,000–99,000 live cells.

To count MGE-derived interneurons, we used GFP-labeled donor cells and tissue slices stained with DAPI or antibodies recognizing GAD67 or PV, which clearly demarcate neocortical layers. For Fig. 1, GFP⁺ cells were counted in layers 1, 2/3, 4, 5 and 6 and the percentage of total GFP⁺ cells in each layer was calculated. For Figs. 2 and 3, GFP⁺ cells and cells colabelled for GFP and PV or SOM were counted in layers 1, 2/3, 4, 5 and 6. The percentage of total GFP⁺ cells in each layer that also expressed PV or SOM was calculated. For each brain, percentages were averaged for several slices and data are reported as mean ± standard error. As expected [18], histological sections close to the injection site contained more GFP⁺ cells whereas those farther away contained fewer cells. Sections of somatosensory cortex 0.75–1.25 mm rostral or caudal to the injection site were used for cell counts.

2.4. Immunohistochemistry and confocal microscopy

Brains were fixed in 4% paraformaldehyde (PFA) by perfusion and 50 μm coronal sections were cut by vibratome. Floated sections were colabeled for GFP (Aves Labs GFP-1020; 1:500) and one of the following: GAD67 (Millipore MAB5406; 1:500), PV (Sigma P3088; 1:500), somatostatin (SOM, Santa Cruz 7819; 1:500), neuropeptide Y (NPY, ImmunoStar 22,940; 1:500) or calretinin (CR; Millipore AB5054; 1:500). Secondary antibodies were Alexa Fluor anti-chicken 488, anti-mouse 594 and anti-rabbit 594 (Molecular Probes; 1:1000). For SOM labeling, slices were first stained with SOM primary overnight, incubated with anti-goat 594 then stained for GFP. All antibodies were incubated in PBS containing 0.05–1% Triton-X 100, 1% bovine serum albumin (BSA; Sigma) and 10% normal goat or donkey serum (Sigma). PBS containing 0.05% Triton-X 100 was used for all intermediate washing steps. Vectashield containing DAPI was used to mount slices (Vector Labs).

To count endogenous and grafted cells, tiled confocal images were acquired at 10× magnification using a Nikon spinning disk and NIS Elements software (Technical Instruments) or 20× magnification using a Leica SP5 confocal and LAF software (Leica). Images were taken 750–1250 μm rostral and caudal to the injection site and cells in each neocortical layer were counted in Image J or Adobe Photoshop. For each stain, several slices from each brain were imaged and used to count cells. Two-way ANOVA were used to test significance (SigmaPlot 12.0, Systat Software Inc.).

3. Results

Previous studies demonstrated that transplanted E12.5 MGE progenitors primarily differentiate into PV⁺ and SOM⁺ interneurons [18,20], but did not examine precisely how these sub-populations are distributed in the recipient neocortex. To address this issue, we first examined the neocortical laminar positioning of grafted GFP⁺ cells in each of the neocortical layers with a focus on somatosensory cortex. Based on previous reports that GABA_BRs facilitate interneuronal migration into the cortical plate [15], we also grafted GFP⁺ MGE cells derived from GABA_{B1}R KO. Functional GABA_BRs cannot form in the absence of either the GABA_BR B1 subunit that contains the ligand binding site [21] or the B2 subunit that is required for membrane expression of the receptor [22]. Tissue sections were processed with antibodies recognizing GFP and GAD67 (Fig. 1A–C). At 30–40 DAT, a significant percentage of the MGE-derived GFP⁺ cells from both WT and GABA_{B1}R KO embryos are distributed in layers L2/3, 5 and 6 (Fig. 1E). Of the WT grafted GFP⁺ cells counted in 8 graft recipients, 5 ± 1%, 34 ± 3%, 6 ± 1%, 18 ± 1% and 37 ± 2% were in L1, 2/3, 4, 5 and 6, respectively. MGE-derived interneurons from GABA_{B1}R KO mice (n = 5) exhibit a similar distribution with 8 ± 3%, 37 ± 5%, 9 ± 2%, 19 ± 5% and 46 ± 5% GFP⁺ cells in L1, 2/3, 4, 5 and 6, respectively. For both WT and KO grafted cells, the

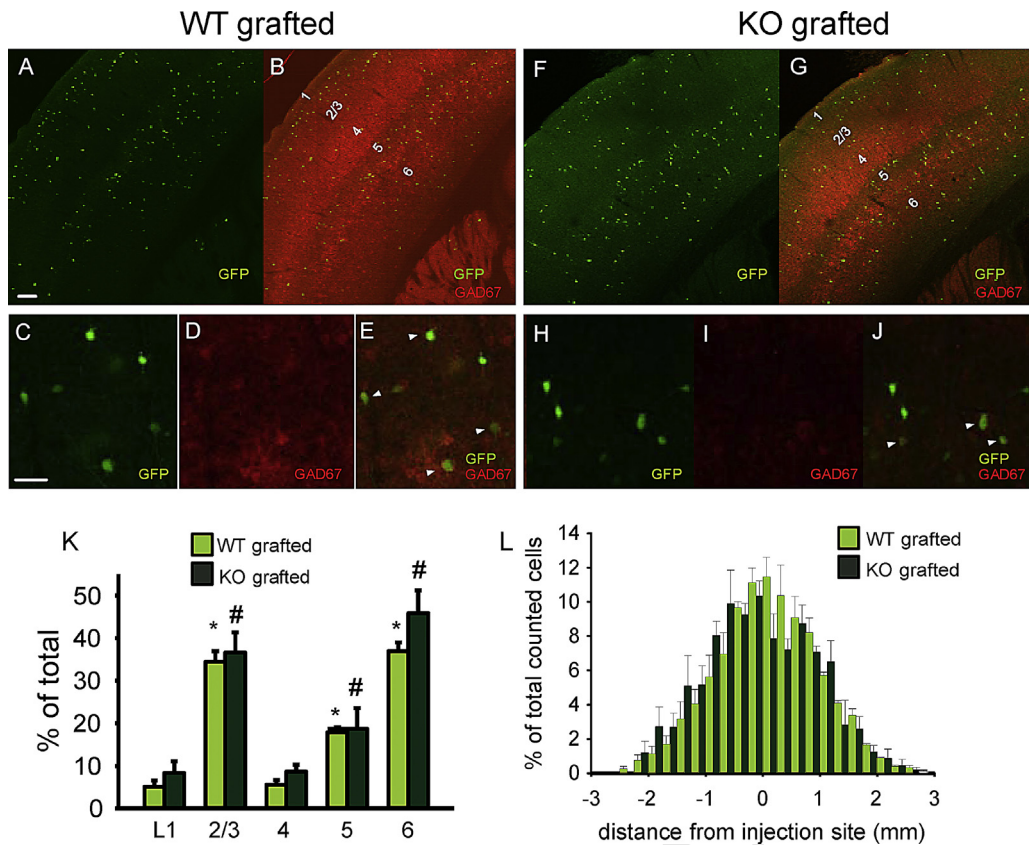


Fig. 1. Transplanted MGE-derived interneurons exhibit layer preference within the host neocortex. Representative images of (A) WT GFP⁺ grafted cells and a merged image of (B) GFP and GAD67 staining 1 mm rostral to injection site. KO GFP⁺ grafted cells (F) and a merged image (G) 1 mm caudal to the injection site. Scale bar = 100 μm. Higher magnification images from separate brain slices show WT (C-E) and KO (H-J) grafted cells, GAD67 staining and merged images in L6. Scale bar = 50 μm. (K) The percent of total counted GFP⁺ cells by layer show that majority of GFP⁺ cells are localized in L2/3, 5 and 6 while grafted cells are relatively sparse in L1 and 4 (WT: n = 8; KO: n = 5). For both WT and KO grafted cells, the % of total counted cells is statistically greater in L2/3 than in L1, 4, and 5, greater in L6 than in L1, 4 and 5 and statistically different in L5 relative to all other layers. Two way ANOVA, Holm-Sidak's test. *, #: see main text for p-values for each interaction. L. WT vs. KO cells exhibit no differences in the rostral to caudal distribution of GFP⁺ cells away from the injection site.

178 percent of total counted cells is statistically greater in L2/3 than
179 in L1, 4, and 5 (*, #: $p < 0.001$), greater in L6 than in L1, 4 and 5
180 (*, #: $p < 0.001$) and statistically different in L5 relative to all
181 other layers (L5 vs. L1, 4: $p < 0.01$; L5 vs. L2/3, 6: $p < 0.001$). In Fig. 1E,

the * and # indicate that the percent of total counted cells in the
marked neocortical layer is statistically different from that in other
layers. However, within each neocortical layer, there was no significant
difference in the laminar positioning of WT vs. GABA_{B1} R KO

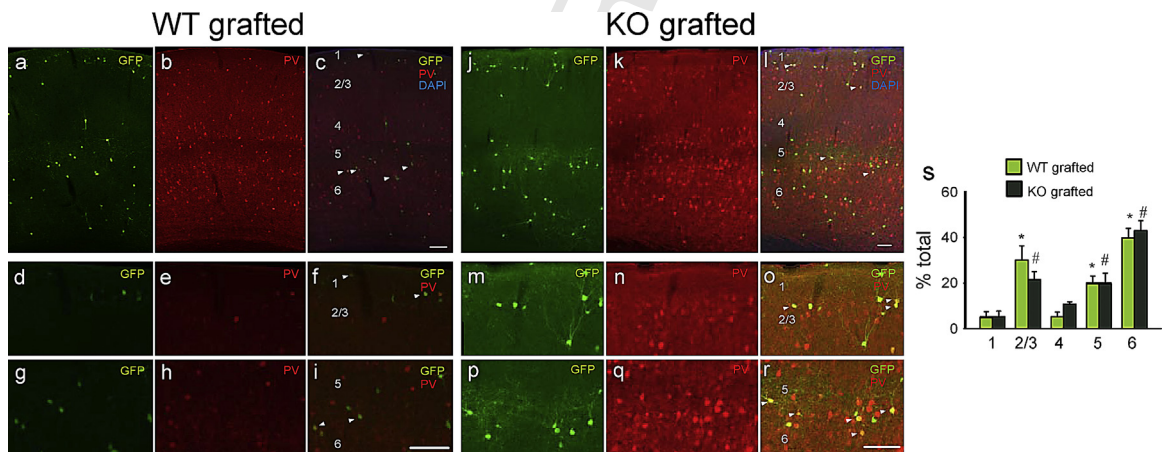


Fig. 2. Laminar distribution of grafted PV⁺ interneurons. A panel of images of the host brain neocortex show GFP⁺ grafted cells (a, j), PV⁺ cells (b, k) and merged images of GFP, PV and DAPI staining (c, l) at low magnification. On the left (a-i) and right (j-r), are images from host mice that received WT and KO MGE cells. All images are 1.0 mm rostral or caudal to injection site (g and h). (d-i: WT graft recipient and m-r: KO graft recipient) higher magnification images taken from the same slices in a and j show the distribution of GFP⁺ and PV⁺ cells and merged images in L1 and 2/3 vs. L5 and 6. Summary histograms (s) show the percent of total counted WT grafted (light green) or KO grafted (dark green) cells in each layer. The percentage of total cells in L2/3, for both WT and KO grafted cells is statistically different than in all other layers. The same is true for L6. Two-way ANOVA, Holm-Sidak posthoc test. * and # indicate statistical significance. See main text for p-values. WT grafted: (n = 6); KO grafted: PV (n = 5). For all images, scale bar = 100 μm. (For interpretation of the references to color in this figure legend, the reader is referred to the web version of the article.)

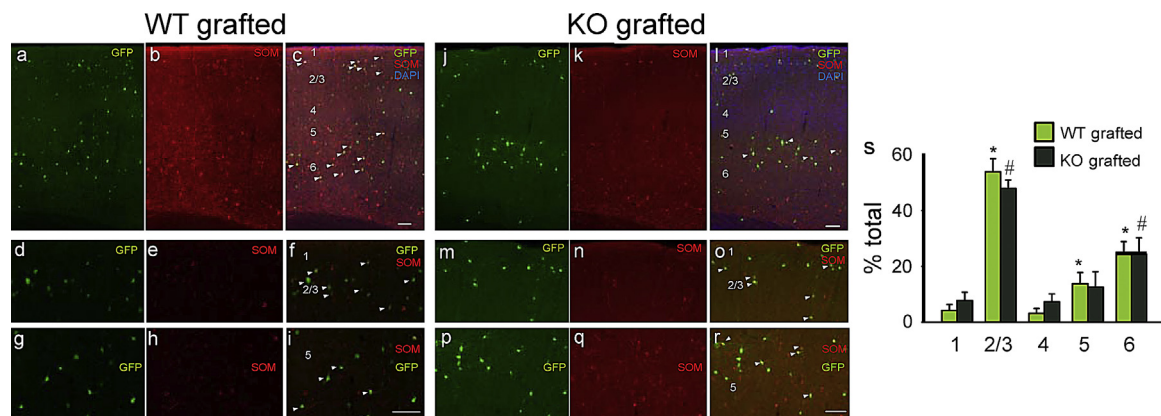


Fig. 3. Laminar distribution of grafted SOM⁺ interneurons. A panel of images of the host brain neocortex show GFP⁺ grafted cells (a, j), SOM⁺ cells (b, k) and merged images of GFP, PV and DAPI staining (c, l) at low magnification. On the left (a–i) and right (j–r), are images from host mice that received WT and KO MGE cells. All images are 1.0 mm rostral or caudal to injection site (g and h). (d–i: WT graft recipient and m–r: KO graft recipient) higher magnification images taken from the same slices in a and j show the distribution of GFP⁺ and SOM⁺ cells and merged images in L1 and 2/3 vs. L5 and 6. Summary histograms (s) show the percent of total counted WT grafted (light green) or KO grafted (dark green) cells in each layer. The percent of WT and KO grafted cells in L2/3 is statistically different than in all other layers. In L6, the percent of WT grafted cells is statistically different than in all other layers and the percent of KO grafted cells is different relative to all layers except L5. Two-way ANOVA, Holm–Sidak posthoc test. See main text for *p* values. WT grafted: (*n* = 5); KO grafted: SOM (*n* = 4). For all images, scale bar = 100 μm. (For interpretation of the references to color in this figure legend, the reader is referred to the web version of the article.)

MGE-derived interneurons. As previously shown [18], MGE progenitors can migrate up to 3 mm from the injection site (Fig. 1F). The normalized migration of WT and GABA_B1R KO MGE-derived interneurons along the rostral to caudal axis relative to injection site was not statistically significant (Fig. 1F).

Next, we evaluated the laminar distribution of MGE-derived PV⁺ and SOM⁺ cells in the recipient neocortex. We co-labeled slices from recipient mice with antibodies recognizing GFP, and either PV or SOM (as well as DAPI) and performed cell counts in somatosensory cortex [18]. Similar to the distribution of total grafted GFP⁺ cells, MGE-derived PV⁺ cells were preferentially located in L2/3, 5 and 6 (Fig. 2). Data represent PV⁺ grafted cells derived from WT donors (host mice = 7) vs. GABA_B1R KO donors (host mice = 5). As shown in Fig. 2s, the percent of total WT MGE-derived cells in L2/3 (30 ± 6%) is statistically different than in L1 (5 ± 3%; *p* < 0.01), L4 (5 ± 2%; *p* < 0.01), L5 (20 ± 3%; *p* < 0.05) and L6 (40 ± 4%; *p* < 0.05) and in L5 relative to L1 (*p* < 0.001), 2/3 (*p* < 0.05) and 4 (*p* < 0.001). The percentage of WT MGE-derived PV⁺ cells in L6 was greater than all other layers (*p* < 0.001). The percentage of GABA_B1R KO MGE-derived PV⁺ cells in L2/3 (22 ± 4%) was statistically different than in L1 (5 ± 3%), L4 (11 ± 1%), L5 (20 ± 5%) and L6 (43 ± 4%) (L2/3 vs. all layers: *p* < 0.001). There were no statistical differences in the percentages of MGE-derived WT vs. GABA_B1R KO PV⁺ cells in each layer.

Similarly MGE-derived SOM⁺ cells were preferentially located in L2/3, 5 and 6 (Fig. 3). Data represent SOM⁺ grafted cells derived from WT donors (host mice = 6) vs. GABA_B1R KO donors (host mice = 4). As shown in Fig. 3s, the percentage of WT MGE-derived SOM⁺ cells in L2/3 (54 ± 5%) was greater than in L1 (4 ± 2%), L4 (3 ± 2%), L5 (14 ± 4%) and L6 (25 ± 4%) (L2/3 vs. all other layers: *p* < 0.001). The percent of total WT MGE-derived cells in L5 was statistically different relative to L1 (*p* < 0.05), L2/3 (*p* < 0.001), L4 (*p* < 0.05) and L6 (*p* < 0.05). The percent of total WT MGE-derived cells in L6 was statistically different relative to L1 (*p* < 0.001, L2/3 (*p* < 0.001), L4 (*p* < 0.001) and L5 (*p* < 0.05). The percentage of GABA_B1R KO MGE-derived SOM⁺ cells in L2/3 (48 ± 3%) was greater than in L1 (8 ± 3%), L4 (7 ± 3%), L5 (13 ± 5%) and L6 (24 ± 6%) (L2/3 vs. all other layers: *p* < 0.001). Again, there were no statistical differences in the percentages of MGE-derived WT vs. GABA_B1R KO SOM⁺ cells in each layer. We have not plotted the distribution of GFP⁺ that also labeled for NPY or CR because only 2% (45 out of 1888 cells) and 1% (16 out of 1363 cells) of the total counted WT MGE-derived cells co-labeled

for these markers making meaningful comparisons difficult. In contrast and consistent with an MGE lineage, 25% and 35% of total counted WT MGE-derived cells co-labeled for PV (473 out of 1875 cells) and SOM (422 out of 1192 cells), respectively.

4. Discussion

Consistent with prior studies [18,23], we show here that grafting immature progenitor cells from embryonic MGE into the postnatal cortex results in GABAergic interneurons that migrate widely in the recipient brain. The main findings of these studies are that (i) MGE-derived interneurons are most prominent in layers 2/3, 5 and 6, (ii) parvalbumin⁺ and somatostatin⁺ neurons comprise the primary interneuron sub-populations derived from MGE progenitors, and (iii) GABA_B1 receptors are not necessary for the migration and final laminar distribution of graft-derived interneurons in the recipient neocortex.

Cortical interneurons migrate tangentially from MGE and CGE [3,4], course through the subventricular and marginal zones of the immature cortex before they enter the cortical plate. In the mouse MGE, this process begins around E9.5 and peaks at E13.5 [24]; CGE migration initiates at E12.5. Within neocortex, interneuron and projection neurons follow an inside-out migration pattern in which earlier born neurons migrate to the deeper layers (L4–6) while later born neurons make their way to superficial layers (L1–3). Mitotic age may influence the laminar position of interneurons to the extent that early-born MGE cells receive different cues from developing neocortex than later-born CGE cells. However, when MGE progenitor cells are transplanted into postnatal neocortex, as in this study, graft-derived cells appear to receive migratory cues that direct them to both superficial and deep neocortical layers. This is consistent with recent findings by Ciceri et al. [17] suggesting that MGE progenitors give rise to interneurons that populate the infra- and supragranular layers of neocortex.

MGE-derived progenitors, which are the focus of the current work receive a wide range of molecular cues that regulate their transition from tangential to radial migration as well as their laminar position within the neocortex [25]. Chemokine signaling mediated by Cxcr4 and Cxcr7 receptors regulates the timing of interneuronal progenitor entry into the cortical plate [26] and laminar positioning in the embryonic and postnatal neocortex [27,28]. In vitro analysis of interneuronal progenitor migration has

demonstrated that GABA_A, acting on ionotropic GABA_ARs, promotes cell motility when the chloride reversal potential (E_{Cl}) is depolarized. However, forced up-regulation of the KCl co-transporter KCC2 hyperpolarizes the E_{Cl} and reduces interneuron motility [11]. These studies indicate that the GABA_AR-mediated efflux or influx of Cl^- can differentially regulate interneuron movement. In contrast to ionotropic GABA_A and GABA_C receptors, metabotropic GABA_BRs hyperpolarize the cell by triggering the efflux of K^+ . Therefore, MGE progenitors derived from GABA_BR KO mice are not susceptible to the regulation of cell motility mediated by changes in KCC2 expression and, subsequently, E_{Cl} . Given that we have exclusively looked at the laminar distribution of interneuron progenitors transplanted into postnatal cortex, further work is necessary to determine whether the neocortical distribution of endogenous interneurons subtypes is disrupted in mice lacking functional GABA_BRs.

Given that neocortical cells in each layer exhibit distinct connectivity patterns, the layer preference of graft-derived interneurons may influence inhibition in some brain regions more than others. Pyramidal cells in layers 2/3, 5 and 6, where the majority of graft-derived MGE cells migrate, send axonal outputs to the contralateral hemisphere (L2/3 and 5) [29] or outside of the neocortex, innervating thalamus, pons, superior colliculus and spinal cord (L5) or thalamus and lateral geniculate nucleus (L6) [30]. By localizing to L2/3, 5 and 6, graft-derived interneurons may maximize their effect on the contralateral hemisphere and to brain regions outside of the neocortex that both receive sensory inputs and execute motor function.

Prior to the formation of inhibitory synapses, GABA is secreted from developing neurons [31] and can promote interneuron migration via the activation of GABA receptors [32–34]. At the earliest age examined (embryonic day 14, E14), the mantle region of the ganglionic eminence as well as tangentially migrating cells of the intermediate zone express GABA_{B1}Rs. By E16, the B1 and B2 subunits of the GABA_BR, both of which are necessary to form functional receptors, are expressed and co-localized in the neocortical primordium and 97% of tangentially migrating neurons also express GABA_{B1}Rs [12]. In addition to immunohistochemical evidence that GABA_BRs are expressed in migrating interneuron progenitors, *in vitro* assays indicate that GABA_B receptor activation facilitates the migration and entry of MGE progenitor cells into the cortical plate [13–16].

5. Conclusions

Our studies suggest that the rostral to caudal and laminar migration of interneuronal progenitors transplanted into the postnatal neocortex does not require functional GABA_BRs.

Acknowledgments

We would like to thank M. Howard and R. Hunt for helpful discussions. This work was supported by funds from the NIH (R01 NS071785 to S.C.B.; F32 NS061497 to J.Y.S.) and the California Institute of Regenerative Medicine (TR2–01749 to A.A.-B.).

References

- [1] O. Yizhar, L.E. Fenno, M. Prigge, F. Schneider, T.J. Davidson, D.J. O'Shea, V.S. Sohal, I. Goshen, J. Finkelstein, J.T. Paz, K. Stehfest, R. Fudim, C. Ramakrishnan, J.R. Huguenard, P. Hegemann, K. Deisseroth, Neocortical excitation/inhibition balance in information processing and social dysfunction, *Nature* 477 (2011) 171–178.
- [2] S.A. Anderson, D.D. Eisenstat, L. Shi, J.L. Rubenstein, Interneuron migration from basal forebrain to neocortex: dependence on *Dlx* genes, *Science* 278 (1997) 474–476.
- [3] O. Marin, J.L. Rubenstein, A long, remarkable journey: tangential migration in the telencephalon, *Nat. Rev. Neurosci.* 2 (2001) 780–790.
- [4] Q. Xu, I. Cobos, E. De La Cruz, J.L. Rubenstein, S.A. Anderson, Origins of cortical interneuron subtypes, *J. Neurosci.* 24 (2004) 2612–2622.
- [5] S. Nery, G. Fishell, J.G. Corbin, The caudal ganglionic eminence is a source of distinct cortical and subcortical cell populations, *Nat. Neurosci.* 5 (2002) 1279–1287.
- [6] D. Gelman, A. Griveau, N. Dehorter, A. Teissier, C. Varela, R. Pla, A. Pierani, O. Marin, A wide diversity of cortical GABAergic interneurons derives from the embryonic preoptic area, *J. Neurosci.* 31 (2011) 16570–16580.
- [7] C. Faux, S. Rakic, W. Andrews, J.M. Britto, Neurons on the move: migration and lamination of cortical interneurons, *Neurosignals* 20 (2012) 168–189.
- [8] D.D. Wang, A.R. Kriegstein, Defining the role of GABA in cortical development, *J. Physiol.* 587 (2009) 1873–1879.
- [9] J.J. LoTurco, D.F. Owens, M.J. Heath, M.B. Davis, A.R. Kriegstein, GABA and glutamate depolarize cortical progenitor cells and inhibit DNA synthesis, *Neuron* 15 (1995) 1287–1298.
- [10] S.Z. Young, M.M. Taylor, S. Wu, Y. Ikeda-Matsuo, C. Kubera, A. Bordey, NKCC1 knockdown decreases neuron production through GABA(A)-regulated neural progenitor proliferation and delays dendrite development, *J. Neurosci.* 32 (2012) 13630–13638.
- [11] D. Bortone, F. Polleux, KCC2 expression promotes the termination of cortical interneuron migration in a voltage-sensitive calcium-dependent manner, *Neuron* 62 (2009) 53–71.
- [12] G. Lopez-Bendito, R. Shigemoto, A. Kulik, O. Paulsen, A. Fairen, R. Lujan, Expression and distribution of metabotropic GABA receptor subtypes GABABR1 and GABABR2 during rat neocortical development, *Eur. J. Neurosci.* 15 (2002) 1766–1778.
- [13] T. Behar, Y. Li, H. Tran, W. Ma, V. Dunlap, C. Scott, J. Barker, GABA stimulates chemotaxis and chemokinesis of embryonic cortical neurons via calcium-dependent mechanisms, *J. Neurosci.* 16 (1996) 1808–1818.
- [14] T. Behar, A. Schaffner, C. Scott, C. O'Connell, J. Barker, Differential response of cortical plate and ventricular zone cells to GABA as a migration stimulus, *J. Neurosci.* 18 (1998) 6378–6387.
- [15] T. Behar, S. Smith, R. Kennedy, J. McKenzie, I. Maric, J. Barker, GABA(B) receptors mediate motility signals for migrating embryonic cortical cells, *Cereb. Cortex* 11 (2001) 744–753.
- [16] K.N. Brown, S. Chen, Z. Han, C.H. Lu, X. Tan, X.J. Zhang, L. Ding, A. Lopez-Cruz, D. Saur, S.A. Anderson, K. Huang, S.H. Shi, Clonal production and organization of inhibitory interneurons in the neocortex, *Science* 334 (2011) 480–486.
- [17] G. Ciceri, N. Dehorter, I. Sols, J.Z. Huang, M. Maravall, O. Marin, Lineage-specific laminar organization of cortical GABAergic interneurons, *Nat. Neurosci.* (2013).
- [18] M. Alvarez-Dolado, M. Calcagnotto, K. Karkar, D. Southwell, D. Jones-Davis, R. Estrada, J. Rubenstein, A. Alvarez-Buylla, S. Baraban, Cortical inhibition modified by embryonic neural precursors grafted into the postnatal brain, *J. Neurosci.* 26 (2006) 7380–7389.
- [19] V. Schuler, C. Luscher, C. Blanchet, N. Klix, G. Sansig, K. Klebs, M. Schmutz, J. Heid, C. Gentry, L. Urban, A. Fox, W. Spooren, A.L. Jaton, J. Vigouret, M. Pozza, P.H. Kelly, J. Mosbacher, W. Froestl, E. Kaslin, R. Korn, S. Bischoff, K. Kaupmann, H. van der Putten, B. Bettler, Epilepsy, hyperalgesia, impaired memory, and loss of pre- and postsynaptic GABA(B) responses in mice lacking GABA(B1), *Neuron* 31 (2001) 47–58.
- [20] S.C. Baraban, D.G. Southwell, R.C. Estrada, D.L. Jones, J.Y. Sebe, C. Alfaro-Cervello, J.M. Garcia-Verdugo, J.L. Rubenstein, A. Alvarez-Buylla, Reduction of seizures by transplantation of cortical GABAergic interneuron precursors into Kv1.1 mutant mice, *Proc. Natl. Acad. Sci. U.S.A.* 106 (2009) 15472–15477.
- [21] K. Kaupmann, B. Malitschek, V. Schuler, J. Heid, W. Froestl, P. Beck, J. Mosbacher, S. Bischoff, A. Kulik, R. Shigemoto, A. Karschin, B. Bettler, GABA(B)-receptor subtypes assemble into functional heteromeric complexes, *Nature* 396 (1998) 683–687.
- [22] A.R. Calver, M.J. Robbins, C. Cosio, S.Q. Rice, A.J. Babbs, W.D. Hirst, I. Boyfield, M.D. Wood, R.B. Russell, G.W. Price, A. Couve, S.J. Moss, M.N. Pangalos, The C-terminal domains of the GABA(b) receptor subunits mediate intracellular trafficking but are not required for receptor signaling, *J. Neurosci.* 21 (2001) 1203–1210.
- [23] H. Wichterle, J.M. Garcia-Verdugo, D.G. Herrera, A. Alvarez-Buylla, Young neurons from medial ganglionic eminence disperse in adult and embryonic brain, *Nat. Neurosci.* 2 (1999) 461–466.
- [24] G. Miyoshi, S.J. Butt, H. Takebayashi, G. Fishell, Physiologically distinct temporal cohorts of cortical interneurons arise from telencephalic Olig2-expressing precursors, *J. Neurosci.* 27 (2007) 7786–7798.
- [25] C. Faux, S. Rakic, W. Andrews, J. Britto, Neurons on the move: migration and lamination of cortical interneurons, *Neurosignals* 20 (2012) 168–189.
- [26] R. Stumm, C. Zhou, T. Ara, F. Lazarini, M. Dubois-Dalq, T. Nagasawa, V. Höllt, S. Schulz, CXCR4 regulates interneuron migration in the developing neocortex, *J. Neurosci.* 23 (2003) 5123–5130.
- [27] J.A. Sanchez-Alcaniz, S. Haegel, W. Mueller, R. Pla, F. Mackay, S. Schulz, G. Lopez-Bendito, R. Stumm, O. Marin, Cxcr7 controls neuronal migration by regulating chemokine responsiveness, *Neuron* 69 (2011) 77–90.
- [28] Y. Wang, G. Li, A. Stanco, J.E. Long, D. Crawford, G.B. Potter, S.J. Pleasure, T. Behrens, J.L. Rubenstein, CXCR4 and CXCR7 have distinct functions in regulating interneuron migration, *Neuron* 69 (2011) 61–76.
- [29] B. Mitchell, J. Macklis, Large-scale maintenance of dual projections by callosal and frontal cortical projection neurons in adult mice, *J. Comp. Neurol.* 482 (2005) 17–32.
- [30] A. Thomson, C. Lamy, Functional maps of neocortical local circuitry, *Front. Neurosci.* 1 (2007) 19–42.

- 415 [31] M. Demarque, A. Represa, H. Becq, I. Khalilov, Y. Ben-Ari, L. Aniksztejn, Paracrine
416 intercellular communication by a Ca²⁺- and SNARE-independent release of
417 GABA and glutamate prior to synapse formation, *Neuron* 36 (2002) 1051–1061. 420
418 [32] T.F. Haydar, F. Wang, M.L. Schwartz, P. Rakic, Differential modulation of prolif- 421
419 eration in the neocortical ventricular and subventricular zones, *J. Neurosci.* 20 422
(2000) 5764–5774. 423
424 [33] G. Lopez-Bendito, R. Lujan, R. Shigemoto, P. Ganter, O. Paulsen, Z. Molnar, Block- 425
ade of GABA(B) receptors alters the tangential migration of cortical neurons, 426
Cereb. Cortex 13 (2003) 932–942. 427
428 [34] J.B. Manent, M. Demarque, I. Jorquera, C. Pellegrino, Y. Ben-Ari, L. Aniksztejn, A. 429
Represa, A noncanonical release of GABA and glutamate modulates neuronal 430
migration, *J. Neurosci.* 25 (2005) 4755–4765. 431

UNCORRECTED PROOF